



# Effects of MgO/Al<sub>2</sub>O<sub>3</sub> ratio on viscous behaviors and structures of MgO–Al<sub>2</sub>O<sub>3</sub>–TiO<sub>2</sub>–CaO–SiO<sub>2</sub> slag systems with high TiO<sub>2</sub> content and low CaO/SiO<sub>2</sub> ratio

Cong FENG<sup>1,2</sup>, Li-hua GAO<sup>1,2</sup>, Jue TANG<sup>1,2</sup>, Zheng-gen LIU<sup>1</sup>, Man-sheng CHU<sup>1,2</sup>

1. School of Metallurgy, Northeastern University, Shenyang 110819, China;

2. State Key Laboratory of Rolling and Automation, Northeastern University, Shenyang 110819, China

Received 22 May 2019; accepted 7 January 2020

**Abstract:** The effects of MgO/Al<sub>2</sub>O<sub>3</sub> ratio on the viscous behaviors of MgO–Al<sub>2</sub>O<sub>3</sub>–TiO<sub>2</sub>–CaO–SiO<sub>2</sub> systems were investigated by the rotating cylinder method. Raman spectroscopy was used to analyze the structural characteristics of slag and Factsage 7.0 was adopted to demonstrate the liquidus temperature of slag. The results show that the viscosity and activation energy for viscous flow decrease when the MgO/Al<sub>2</sub>O<sub>3</sub> ratio increases from 0.82 to 1.36. The break point temperature and liquidus temperature of slag initially decrease and subsequently increase. The complex viscous structures are gradually depolymerized to simple structural units. In conclusion, with the increase of MgO/Al<sub>2</sub>O<sub>3</sub> ratio, the degree of polymerization of slag decreases, which improves the fluidity of slag. The variations of liquidus temperature of slag lead to the same changes of break point temperature.

**Key words:** vanadium-bearing titanomagnetite; titanium-bearing slag; viscous behavior; degree of polymerization of slag; MgO/Al<sub>2</sub>O<sub>3</sub> ratio

## 1 Introduction

Vanadium-bearing titanomagnetite (V–Ti ores) is an important mineral resource containing Fe, V and Ti elements [1,2]. Since 1970s, the traditional blast furnace (BF) process has been employed to process V–Ti ores. The TiO<sub>2</sub> content of titanium-bearing BF slag is only 20–25 wt.% [3]. For the lack of efficient methods to extract the TiO<sub>2</sub> component from the titanium-bearing BF slag, the abundant titanium resources are wasted. Considering the disadvantages of BF process, the direct reduction-electric furnace process has been reported as a simple route to realize the recovery of V and Ti resources from V–Ti ores [4–6]. When the iron and vanadium resources are utilized, the

introductions of impurities are reduced. The TiO<sub>2</sub> grade in the titanium-bearing slag is improved (exceed 40 wt.%) [7]. Subsequently, the appropriate hydrometallurgical process can be adopted to efficiently extract TiO<sub>2</sub> from the titanium-bearing slag, realizing the comprehensive utilizations of V–Ti ores [8,9].

Significantly, the smelting separation of V–Ti ore metalized pellets is the most critical step when the direct reduction-electric furnace process is adopted to maximize the utilizations of V–Ti ores, which controls the distribution ratios of valuable elements between the metal and the slag. It is closely related to the viscous behaviors of slag [10–12]. Therefore, the fundamental researches on the viscous behaviors of titanium-bearing slag obtained in the smelting separation process of V–Ti

**Foundation item:** Projects (51574067, 51904063) supported by the National Natural Science Foundation of China; Projects (N172503016, N172502005, N172506011) supported by Fundamental Research Funds for the Central Universities, China; Project (2018M640259) supported by China Postdoctoral Science Foundation

**Corresponding author:** Man-sheng CHU; Tel: +86-24-83684959; E-mail: [chums@smm.neu.edu.cn](mailto:chums@smm.neu.edu.cn)  
DOI: 10.1016/S1003-6326(20)65255-4

ores are necessary.

The viscous behaviors and structural characteristics of titanium-bearing slag have been researched [13–17]. SHI et al [13] measured the viscosity of  $\text{CaF}_2\text{-CaO-Al}_2\text{O}_3\text{-MgO-(TiO}_2\text{)}$  systems and analyzed the degree of polymerization of slag. They concluded that the degree of polymerization of slag decreased by forming some simple structural units with the increase of  $\text{TiO}_2$  content in the experimental range. Consequently, the viscosity and activation energy for viscous flow of slag decreased. QIU et al [14] reported the effects of  $\text{Cr}_2\text{O}_3$  addition and  $\text{CaO/SiO}_2$  ratio on the viscosity and structure of  $\text{CaO-SiO}_2\text{-Cr}_2\text{O}_3\text{-8wt.\%MgO-22wt.\%TiO}_2\text{-14wt.\%Al}_2\text{O}_3$  systems ( $\text{CaO/SiO}_2$  ratio of 0.90–1.30, and  $\text{Cr}_2\text{O}_3$  content of 0–4 wt.%), in which the viscosity of slag obviously increased with the increase of  $\text{Cr}_2\text{O}_3$  content and decreased with the increase of  $\text{CaO/SiO}_2$  ratio. But the restructure and transformations of various structural units in the titanium-bearing slag have not been discussed in detail. ZHEN et al [15] demonstrated that the degree of polymerization of  $\text{CaO-MgO-Al}_2\text{O}_3\text{-SiO}_2\text{-TiO}_2$  systems increased when the  $\text{Al}_2\text{O}_3/\text{TiO}_2$  ratio increased, resulting in an increase of viscosity. ZHANG et al [16] verified that the  $\text{TiO}_2$  component acted as the basic oxide in the  $\text{CaO-SiO}_2\text{-TiO}_2\text{-8wt.\%MgO-14wt.\%Al}_2\text{O}_3$  system and had a prominent effect on depolymerizing the networks of slag. When the  $\text{TiO}_2$  content increased from 0 to 30 wt.%, the viscosity of slag decreased. In addition, LI et al [17] found that  $\text{Ti}^{4+}$  generated by  $\text{TiO}_2$  component in the molten  $\text{CaO-SiO}_2\text{-TiO}_2\text{-15wt.\%CaF}_2$  slag systems ( $\text{CaO/SiO}_2$  ratio of 1.00, and  $\text{TiO}_2$  content of 0–10 wt.%) mainly existed in  $\text{TiO}_4^{4-}$  in slag and formed the  $\text{TiO}_2$ -like clusters with  $\text{Ti}^{4+}$  in tetrahedral coordination, which could not change the degree of polymerization of networks. A small amount of  $\text{Ti}^{4+}$  entered into the networks as the role of network formation and the degree of polymerization of networks was enhanced. These researches were mainly focused on the titanium-bearing BF slag, mold flux and refining slag. Moreover, the analyzed emphases and results of different slag systems were inconsistent.

Currently, the reports on the viscous behaviors of titanium-bearing slag with low  $\text{CaO/SiO}_2$  ratio (less than 0.80) and high  $\text{TiO}_2$  content (exceed 40 wt.%) were few. In our previous work [18], the

effects of  $\text{CaO/SiO}_2$  ratio on the viscous behaviors of titanium-bearing slag obtained in the smelting separation process of V–Ti ores have been researched. Nevertheless, the effects of  $\text{MgO/Al}_2\text{O}_3$  ratio on the viscous behaviors of this type high- $\text{TiO}_2$ -content slags are not investigated in detail. The variations of degree of polymerization of slag are not clear.

In this study, the effects of  $\text{MgO/Al}_2\text{O}_3$  ratio on the viscous behaviors and structural characteristics of  $\text{MgO-Al}_2\text{O}_3\text{-TiO}_2\text{-CaO-SiO}_2$  systems with high  $\text{TiO}_2$  content of 43 wt.% and the low  $\text{CaO/SiO}_2$  ratio of 0.50 were researched. The viscosity, break point temperature, activation energy for viscous flow and degree of polymerization of slag were analyzed. The range of  $\text{MgO/Al}_2\text{O}_3$  ratio was 0.82–1.36. In addition, Raman spectroscopy was used to analyze the structural characteristics of slag and Factsage 7.0 was adopted to demonstrate the liquidus temperature of slag.

## 2 Experimental

### 2.1 Slag sample preparation

The experimental slag samples were synthesized with the calcined analytical-grade oxides of  $\text{CaO}$ ,  $\text{SiO}_2$ ,  $\text{MgO}$ ,  $\text{Al}_2\text{O}_3$  and  $\text{TiO}_2$  in a molybdenum crucible at 1843 K, based on the approximate compositions of titanium-bearing slag obtained in the practical smelting separation process of V–Ti ores. The main chemical compositions of basic titanium-bearing slag are listed in Table 1. Due to the low content of Fe and V element in the titanium-bearing slag, it has little effects on the viscous behaviors and melting behaviors of slag. Therefore, the Fe and V element were not considered in the process of preparing the sample. The experimental scheme and chemical compositions of titanium-bearing slags with different  $\text{MgO/Al}_2\text{O}_3$  ratios are given in Table 2. The  $\text{TiO}_2$  content is fixed to 43 wt.% and the  $\text{CaO/SiO}_2$  ratio is a constant of 0.50. Because the  $\text{CaO/SiO}_2$  ratio of experimental slags is less than 1.00 and the  $\text{TiO}_2$  component is an amphoteric

**Table 1** Main chemical compositions of basic titanium-bearing slag

Content/wt.%							CaO/SiO <sub>2</sub> ratio
CaO	SiO <sub>2</sub>	MgO	Al <sub>2</sub> O <sub>3</sub>	TiO <sub>2</sub>	Fe	V	
10.65	20.72	11.32	11.22	43.58	1.42	0.15	0.514

oxide, the experimental titanium-bearing slags have the acidic slag characteristics.

## 2.2 Experimental apparatus

The viscosity measurements of experimental slags were carried out by the rotating cylinder method with a digital viscometer. The schematic diagram of apparatus is shown in Fig. 1. Six U-shaped MoSi<sub>2</sub> heating elements were used in the electric resistance furnace to heat and melt the slag samples. The temperature of slag could reach 1843 K. The experimental temperatures were controlled by two B-type thermocouples inserted into the furnace with an error less than  $\pm 3$  K. The crucible and rotating spindle employed for the viscosity measurements were both made of molybdenum. The detailed dimensions are also given in Fig. 1. Before the viscosity measurements of slag, the viscometer was calibrated using the standard castor oil with known viscosity at room temperature. Other detailed descriptions of the above equipment were reported in our previous studies [18–20].

## 2.3 Viscosity measurements

The pre-melted slag sample of  $(140 \pm 0.01)$  g was filled in a molybdenum crucible. The crucible was then placed at the even temperature zone of resistance furnace, when the experimental slags were heated to 1843 K. After the slag sample completely melted, its amount was about 40 mm in depth. It took 30 min to stabilize the temperature and homogenize the compositions of molten slag. Then, the molybdenum rotating spindle was slowly immersed in the molten slag and kept at a distance of 10 mm above the crucible bottom. The crucible and spindle were properly aligned along the axis of viscometer. Subsequently, the viscosity measurements were started. In the whole experimental process, argon gas (purity of 99.99%) was flowed with 0.3 L/min to protect the molybdenum crucible, molybdenum spindle and apparatus.

The viscosity measurements of slag were performed with the continuous cooling method to acquire the relationships between the viscosity and the temperature in a wide temperature range. The

**Table 2** Experimental scheme and chemical compositions of experimental slag samples

No.	Initial designed composition							Final composition by XRF						
	Content/wt.%					CaO/ SiO <sub>2</sub> ratio	MgO/ Al <sub>2</sub> O <sub>3</sub> ratio	Content/wt.%					CaO/ SiO <sub>2</sub> ratio	MgO/ Al <sub>2</sub> O <sub>3</sub> ratio
	CaO	SiO <sub>2</sub>	MgO	Al <sub>2</sub> O <sub>3</sub>	TiO <sub>2</sub>			CaO	SiO <sub>2</sub>	MgO	Al <sub>2</sub> O <sub>3</sub>	TiO <sub>2</sub>		
1	12.33	24.67	9.00	11.00	43.00	0.50	0.82	11.76	24.39	9.26	10.78	43.36	0.48	0.86
2	11.67	23.33	11.00	11.00	43.00	0.50	1.00	11.53	22.61	11.43	11.14	42.79	0.51	1.03
3	11.00	22.00	13.00	11.00	43.00	0.50	1.18	10.62	22.11	12.78	10.56	43.45	0.48	1.21
4	10.33	20.67	15.00	11.00	43.00	0.50	1.36	10.56	20.31	14.78	10.85	43.21	0.52	1.36

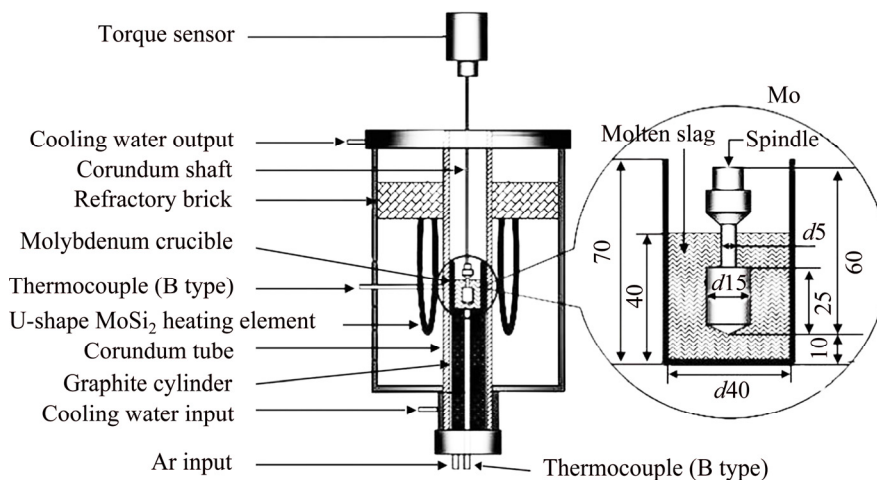


**Fig. 1** Schematic diagram of experimental apparatus (unit: mm)

molten slag was cooled with a rate of 3 K/min from 1843 K. When the viscosity of slag reached about 3.5 Pa·s, the measurements were ended. After the viscosity measurements, the experimental slags were reheated to 1843 K and maintained for 60 min. Subsequently, the reheated molten slags were quenched in the cold water to obtain the amorphous phases for the structural analyses. Further detailed descriptions on the viscosity measurement processes were also illustrated in our previous reports [18–20].

### 3 Results and discussion

#### 3.1 Reproducibility of viscosity measurements

In the present work, the viscosity data of titanium-bearing slags with different MgO/Al<sub>2</sub>O<sub>3</sub> ratio are the average values of measurement results for three times. In order to analyze the reproducibility and accuracy of the viscosity measurements, the comparative results of viscosity measurements for No. 1 experimental slag are given in Table 3. It can be seen that the measured viscosity values at various temperatures are greatly matched. The relative deviations of measured viscosity data from the mean value are less than 1.00%. This illustrates that the viscosity measurement methods adopted in this study are reliable. In addition, the chemical compositions and phases of quenched experimental slags obtained after the viscosity measurements are analyzed by XRF and XRD in Table 2 and Fig. 2. Clearly, the compositions of quenched slags are very similar to the initial designed compositions. The XRD analyses show that all the quenched experimental slags are amorphous and representative of molten state of slag.

**Table 3** Viscosity measurements for No. 1 experimental slag

Temperature/ K	Viscosity measurement/ (Pa·s)	Average viscosity/ (Pa·s)	Relative deviation/ %
1843	0.275, 0.278, 0.275	0.276	0.48
1823	0.297, 0.292, 0.291	0.293	0.80
1793	0.317, 0.322, 0.316	0.318	0.73
1773	0.344, 0.343, 0.340	0.342	0.49
1753	0.373, 0.371, 0.369	0.371	0.36
1733	0.460, 0.462, 0.465	0.462	0.36

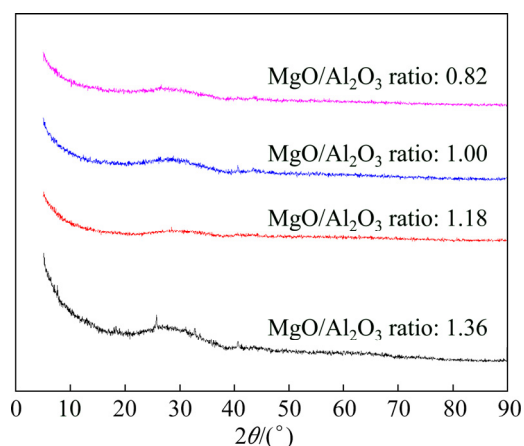


**Fig. 2** XRD patterns of quenched titanium-bearing slags with different MgO/Al<sub>2</sub>O<sub>3</sub> ratio

#### 3.2 Effects of MgO/Al<sub>2</sub>O<sub>3</sub> ratio on break point temperature

Figure 3 displays the viscosity–temperature ( $\eta$ – $T$ ) curves of titanium-bearing slags with different MgO/Al<sub>2</sub>O<sub>3</sub> ratios by the viscosity measurements in the continuous cooling process. It is found that the viscosity of slag gradually increases with a decrease of temperature. When the temperature decreases to a certain value (a temperature turning point), the viscosity of slag has a sharp increase. Generally, this temperature turning point is defined as the break point temperature ( $T_{Br}$ ) of slag. It is also known as the free flow temperature of slag and is an important viscous property of molten slag [21].

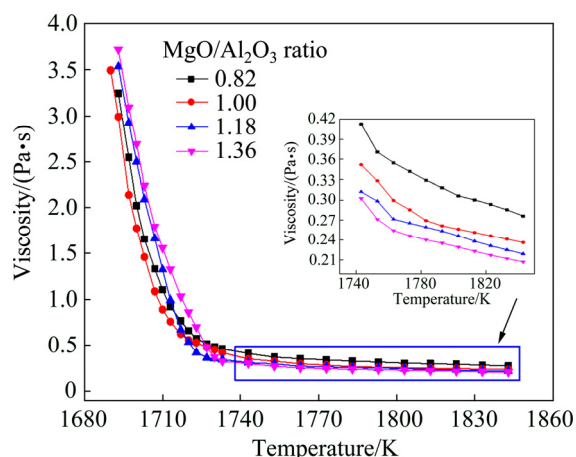


**Fig. 3** Viscosity–temperature ( $\eta$ – $T$ ) curves of titanium-bearing slags with different MgO/Al<sub>2</sub>O<sub>3</sub> ratios

According to the work performed by QI et al [22], the  $T_{Br}$  of slag is determined as the temperature that corresponds to the tangency point

of a 45° line on  $\eta$ - $T$  curve. As illustrated in Fig. 4(a), the  $T_{Br}$  of slags with different MgO/Al<sub>2</sub>O<sub>3</sub> ratios is 1721, 1718, 1723 and 1730 K, which initially decreases and subsequently increases with the increase of MgO/Al<sub>2</sub>O<sub>3</sub> ratio from 0.82 to 1.36.

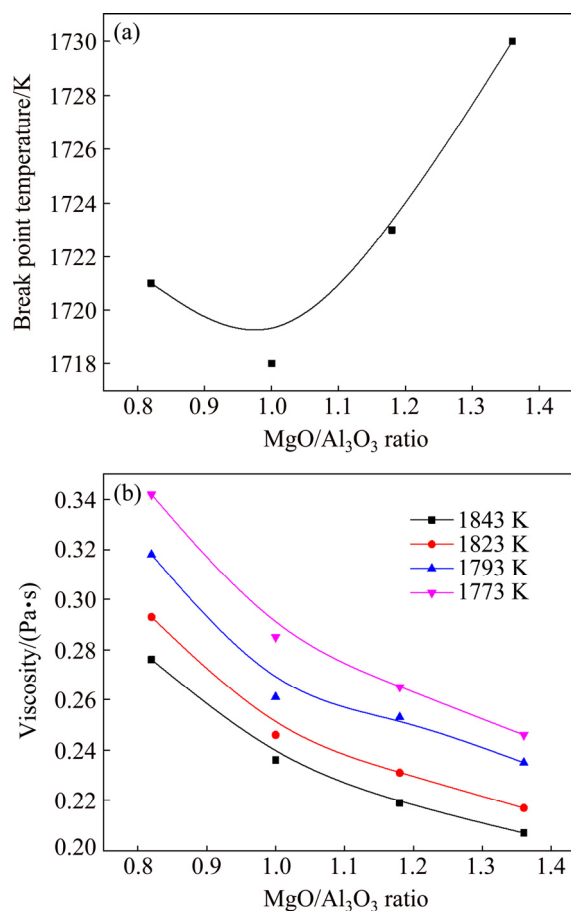


**Fig. 4** Variations of  $T_{Br}$  (a) and viscosity (b) of slags with MgO/Al<sub>2</sub>O<sub>3</sub> ratio

It should be noted that the  $T_{Br}$  is distinguished from the liquidus temperature of slag. The  $T_{Br}$  of slag is the critical temperature where the viscosity of slag changes sharply with the temperature. It can represent the boundary between better fluidity and worse fluidity of slag in one sense. The liquidus temperature of slag refers to the initial point where the solid crystals are precipitated from the molten slag. As reported in the relevant literature, it is still difficult for the acidic slag to flow freely when the slag completely melts, and the viscosity of slag is high. Only when the temperature is further increased to the  $T_{Br}$ , can the acidic molten slag reach the free flow state [23]. Although the  $T_{Br}$  is inconsistent with the liquidus temperature of slag, the variations of  $T_{Br}$  have a relationship with the liquidus temperature of slag [24,25]. Therefore,

Factsage 7.0 was adopted to calculate the phase diagram of MgO–Al<sub>2</sub>O<sub>3</sub>–TiO<sub>2</sub>–CaO–SiO<sub>2</sub> system with the TiO<sub>2</sub> content of 43 wt.% and CaO/SiO<sub>2</sub> ratio of 0.50. Meanwhile, the effects of MgO/Al<sub>2</sub>O<sub>3</sub> ratio on the liquidus temperature of experimental slags were analyzed. The results are shown in Fig. 5. The slag system transfers from the crystalline region of rutile to that of MgTi<sub>2</sub>O<sub>5</sub>, while the MgO/Al<sub>2</sub>O<sub>3</sub> ratio is increased from 0.82 to 1.36. The liquidus temperature of experimental slags calculated by Factsage 7.0 is 1605, 1585, 1607 and 1625 K, respectively, which is initially decreased and subsequently increased. It is same to the variations of  $T_{Br}$ .

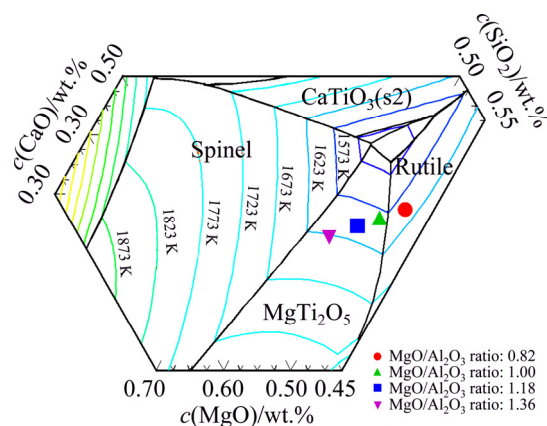


**Fig. 5** Phase diagram of MgO–Al<sub>2</sub>O<sub>3</sub>–43wt.%TiO<sub>2</sub>–CaO–SiO<sub>2</sub> system with CaO/SiO<sub>2</sub> ratio of 0.50

As QI et al [22] noted, when the liquidus temperature of slag is low and the actual temperature is higher than the liquidus temperature, the superheat degree (the difference between the actual temperature  $T$  and the liquidus temperature  $T_L$  of slag, expressed as  $T-T_L$ ) of slag is high. As a result, the slag can keep the molten state more easily in the continuous cooling process from the high temperature to the low temperature, and the sharp increase of viscosity is restrained, contributing to the decrease of  $T_{Br}$ .

### 3.3 Effects of MgO/Al<sub>2</sub>O<sub>3</sub> ratio on viscosity

The viscosities of titanium-bearing slags with different MgO/Al<sub>2</sub>O<sub>3</sub> ratios at various temperatures are shown in Fig. 4(b). The viscosity decreases at given temperatures when the MgO/Al<sub>2</sub>O<sub>3</sub> ratio increases from 0.82 to 1.36. In the molten slag, the SiO<sub>2</sub> component has an obvious characteristic of acid oxide and can produce the complex [SiO<sub>4</sub>]-tetrahedral structures [26,27]. Al<sup>3+</sup> dissociated by

Al<sub>2</sub>O<sub>3</sub> in slag can cause the [AlO<sub>4</sub>]-tetrahedral structures to form and further incorporate into the [SiO<sub>4</sub>]-tetrahedral structures, behaving as a network former [25]. In addition, the TiO<sub>2</sub> component in the molten titanium-bearing slag can generate the complex O—Ti—O deformation in sheet structures [28]. These complex viscous structures can increase the amounts of bridged oxygen (O<sup>0</sup>), which strengthens the degree of polymerization of slag. In the previous works on the correlations between the viscosity and the degree of polymerization of slag, these complex viscous structures had an important influence on the viscosity of slag [29,30]. Their depolymerizations resulted in the lower viscosity of slag.

In the molten slag, MgO can be dissociated to Mg<sup>2+</sup> and free oxygen ions O<sup>2-</sup>. As the MgO/Al<sub>2</sub>O<sub>3</sub> ratio increases, more free oxygen ions O<sup>2-</sup> are provided to the slag. These O<sup>2-</sup> can react with O<sup>0</sup> in the complex viscous networks to produce the non-bridged oxygen (O<sup>-</sup>) [31]. Therefore, the increase of MgO/Al<sub>2</sub>O<sub>3</sub> ratio results in the increasing of polymerization degree of slag and the increasing of the viscosity of experimental slags.

### 3.4 Effects of MgO/Al<sub>2</sub>O<sub>3</sub> ratio on activation energy for viscous flow

The activation energy for viscous flow ( $E_\eta$ ) is an important viscous characteristic of slag. It can reflect the fluctuation degree of viscosity with the temperature change and represent the thermal stability of slag. In addition, it is an indication of energy required to sever a sufficient number of bonds within the networks to initiate flow. Variations of  $E_\eta$  reveal the changes of frictional resistance for viscous flow and suggest a change of structural units in the molten slag. Unless the characteristics of structural units in slag change, the value of  $E_\eta$  is expected to be constant for a certain molten slag [22,25]. This value can be obtained from the Arrhenius equation, combining the linear regression method and viscosity data above the  $T_{Br}$ . The Arrhenius type equation is shown as [22]

$$\ln \frac{\eta}{T} = \ln A + \frac{E_\eta}{R} \cdot \frac{1}{T} \quad (1)$$

where  $\eta$  is the viscosity of slag, Pa·s;  $A$  is the proportionality constant;  $T$  is the temperature, K;  $R$  is the gas constant (8.314 J/(mol·K));  $E_\eta$  is the activation energy for viscous flow, J/mol.

Figure 6(a) presents  $\ln(\eta/T)$  as a function of

$1/T$  for titanium-bearing slags with different MgO/Al<sub>2</sub>O<sub>3</sub> ratios. It can be seen that  $\ln(\eta/T)$  has a good linear relationship with  $1/T$  and the linearly dependent coefficient  $r$  is higher than 0.95 for all slags. These results indicate that the relationships between viscosity and temperature are closely consistent with the Arrhenius behaviors.

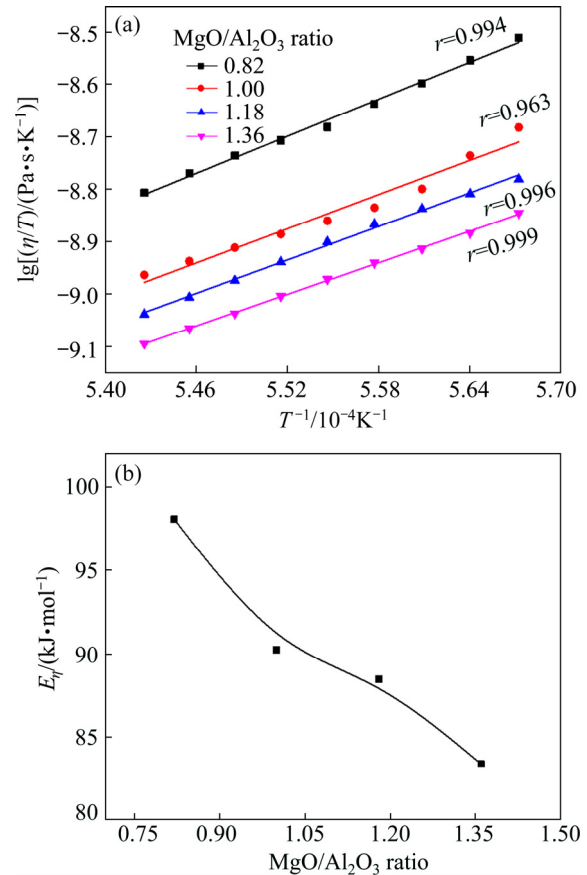


**Fig. 6** Linear fitting between  $\ln(\eta/T)$  and  $T^{-1}$  (a), and variations of  $E_\eta$  of slags with different MgO/Al<sub>2</sub>O<sub>3</sub> ratios (b)

Based on the above experimental data,  $E_\eta$  of slag are obtained through the slope of fitting line. The effects of MgO/Al<sub>2</sub>O<sub>3</sub> ratio on the  $E_\eta$  of slag are calculated and plotted in Fig. 6(b). The  $E_\eta$  decreases from 98.08 to 83.36 kJ/mol with the increase of MgO/Al<sub>2</sub>O<sub>3</sub> ratio from 0.82 to 1.36, which is similar to the variations of viscosity. The decrease of  $E_\eta$  implies that the energy barrier for viscous flow is reduced and the structural units for viscous flow become simpler with an increase of MgO/Al<sub>2</sub>O<sub>3</sub> ratio.

### 3.5 Raman spectra analyses on degree of polymerization of slag

In order to obtain the structural characteristics

of molten titanium-bearing slags and further reveal the variation mechanisms of viscosity and activation energy for viscous flow, Raman spectroscopy was adopted to analyze the amorphous quenched slags. Figure 7(a) shows the original Raman spectra of experimental slags in the

range of  $400\text{--}1200\text{ cm}^{-1}$ . It can be seen that, a strong band exists in the region between  $500$  and  $950\text{ cm}^{-1}$ . With the increase of  $\text{MgO}/\text{Al}_2\text{O}_3$  ratio, this strong band becomes more pronounced. Besides, a shoulder band is observed in the range of  $950\text{--}1100\text{ cm}^{-1}$  at the  $\text{MgO}/\text{Al}_2\text{O}_3$  ratio of  $0.82$ .

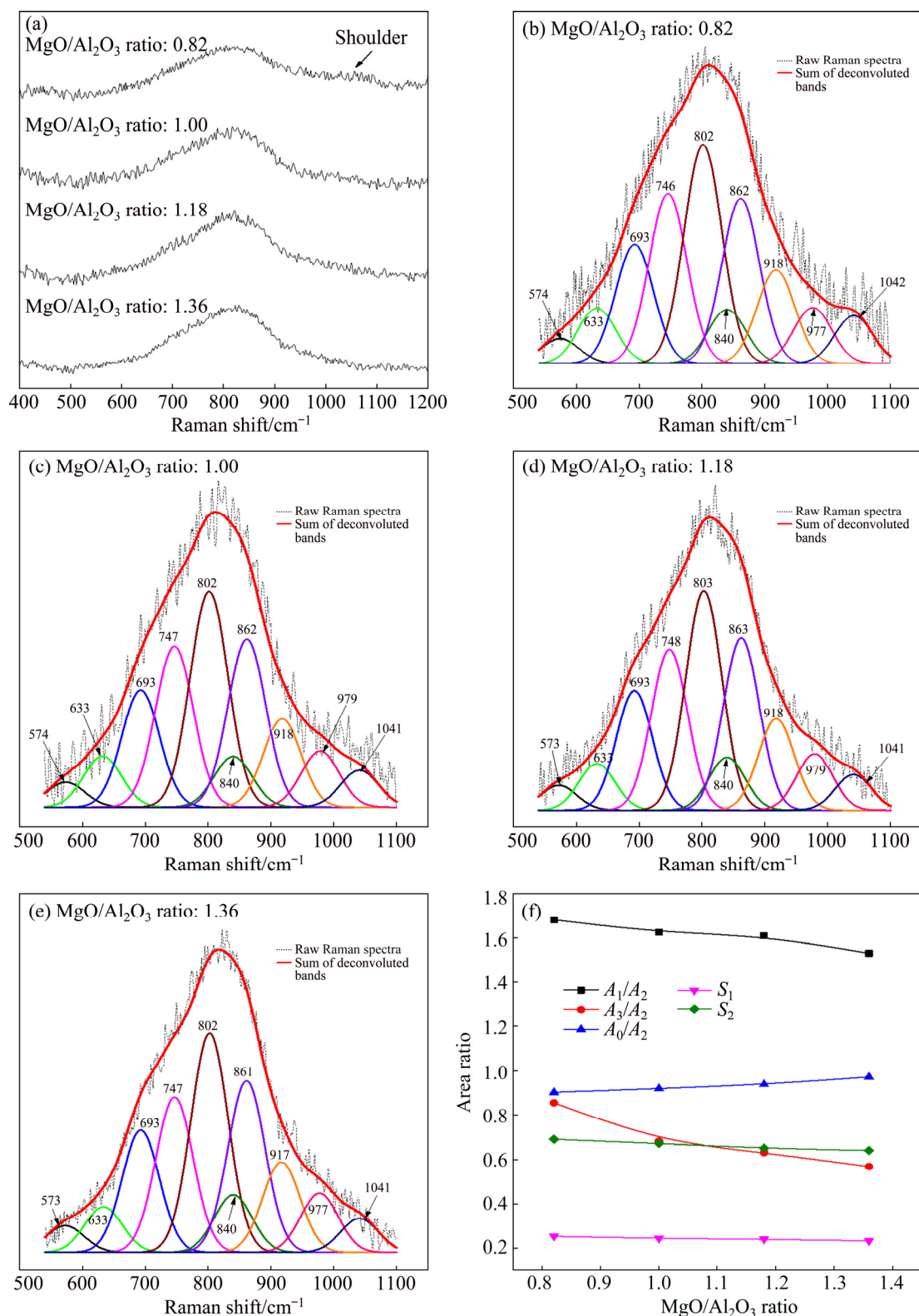


**Fig. 7** Raman spectra (a), deconvolution results (b–e) and further analyses (f) for slags with different  $\text{MgO}/\text{Al}_2\text{O}_3$  ratios

And the corresponding shoulder almost disappears as the MgO/Al<sub>2</sub>O<sub>3</sub> ratio further reaches 1.36.

The conversions of various structural units in the molten slag with the MgO/Al<sub>2</sub>O<sub>3</sub> ratio can be speculated by the deconvolutions of Raman spectra [32]. According to the obvious distributions of bands in the spectra, the focus of deconvolutions in this work is in the 550–1100 cm<sup>-1</sup> range. The obtained Raman spectra are deconvoluted by Gaussian-deconvolution method and the deconvolution fitting process was conducted under the guidance of works performed by JIN et al [33]. The deconvoluted results of Raman spectra of titanium-bearing slags with different MgO/Al<sub>2</sub>O<sub>3</sub> ratios are illustrated in Figs. 7(b–e). Ten deconvolution bands are presented in the analyzed frequency range to be about 570, 630, 690, 750, 800, 840, 860, 920, 980 and 1040 cm<sup>-1</sup>, respectively.

The structural units of TiO<sub>2</sub>-free silicate have been reported by Raman spectroscopy in many studies. The band at 840–860 cm<sup>-1</sup> is due to the stretching vibrations of silicate tetrahedral with four non-bridged oxygen (NBO) and it is referred to  $Q_{Si}^0$  (superscript refers to the number of bridged oxygen) species in monomer structure. The bands located at 900–920, 960–980 and ~1040 cm<sup>-1</sup> correspond to  $Q_{Si}^1$  in the dimer structure,  $Q_{Si}^2$  in the chain structure and  $Q_{Si}^3$  in the sheet structure, respectively [34]. Al<sup>3+</sup> can form as different structural units in the molten slag, where [AlO<sub>4</sub>]-tetrahedral stretching vibration acts as network former and [AlO<sub>6</sub>]-octahedron stretching vibration plays a network modifier. According to JUNG and SOHN [35], Raman band at about 570 cm<sup>-1</sup> is assigned to the [AlO<sub>6</sub>]-octahedron and Raman band at about 630 cm<sup>-1</sup> represents the [AlO<sub>4</sub>]-tetrahedral. In addition, MYSEN et al [36], PARK et al [37], ZHEN et al [15] and WANG et al [38] have suggested that the bands at 860–880, 790–830, 720–750 and 690–700 cm<sup>-1</sup> on the Raman spectra of titanium-bearing melts are due to the Ti—O stretching vibrations in Ti<sub>2</sub>O<sub>6</sub><sup>4-</sup> chain structure, Ti—O stretching vibrations in TiO<sub>4</sub><sup>4-</sup> monomer structure, O—Ti—O deformation in sheet structure and Ti—O stretching vibrations in 6-coordinated Ti<sup>4+</sup>, respectively. The O—Ti—O deformation in sheet structure is complex structural unit. The TiO<sub>4</sub><sup>4-</sup> monomers, Ti<sub>2</sub>O<sub>6</sub><sup>4-</sup> chains and Ti—O stretching vibrations in 6-coordinated Ti<sup>4+</sup> are simple structural units, decreasing the

polymerization strength of complex viscous structures [39]. A brief summary is given in Table 4. The central band frequency of various structural units in the Raman spectra of experimental slags is displayed in Table 5. The central band frequency of

**Table 4** Assignments of Raman bands on spectra for experimental slags

Raman shift/cm <sup>-1</sup>	Raman assignment	Reference
~570	[AlO <sub>6</sub> ]-octahedron stretching vibrations	[35]
~630	[AlO <sub>4</sub> ]-tetrahedral stretching vibrations	[35]
690–700	Ti—O stretching vibrations in 6-coordinated Ti <sup>4+</sup>	[38]
720–750	O—Ti—O deformation in sheet structures	[36]
790–830	Ti—O stretching vibrations in TiO <sub>4</sub> <sup>4-</sup> monomers	[37, 36, 15]
840–860	SiO <sub>4</sub> <sup>4-</sup> with zero bridging oxygen in monomer units, $Q_{Si}^0$	[34]
860–880	Ti—O stretching vibrations in Ti <sub>2</sub> O <sub>6</sub> <sup>4-</sup> chain units	[36]
900–920	Si <sub>2</sub> O <sub>7</sub> <sup>6-</sup> with one bridging oxygen in dimer units, $Q_{Si}^1$	[34]
960–980	Si <sub>2</sub> O <sub>6</sub> <sup>4-</sup> with two bridging oxygen in chain units, $Q_{Si}^2$	[34]
1010–1040	Si <sub>2</sub> O <sub>5</sub> <sup>2-</sup> with three bridging oxygen in sheet units, $Q_{Si}^3$	[34, 15]

**Table 5** Central band frequency of various structural units on Raman spectra of experimental slags (cm<sup>-1</sup>)

Structural units	MgO/Al <sub>2</sub> O <sub>3</sub> ratio			
	0.82	1.00	1.18	1.36
$Q_{Si}^0$ in monomer structure	840	840	840	840
$Q_{Si}^1$ in dimer structure	918	918	918	917
$Q_{Si}^2$ in chain structure	977	979	979	977
$Q_{Si}^3$ in sheet structure	1042	1041	1041	1041
[AlO <sub>6</sub> ]-octahedron	574	574	573	573
[AlO <sub>4</sub> ]-tetrahedral	633	633	633	633
Ti—O stretching vibrations in TiO <sub>4</sub> <sup>4-</sup> monomer structure	802	802	803	802
Ti—O stretching vibrations in Ti <sub>2</sub> O <sub>6</sub> <sup>4-</sup> chain structure	862	862	863	861
O—Ti—O deformation in sheet structure	746	747	748	747
Ti—O stretching vibrations in 6-coordinated Ti <sup>4+</sup>	693	693	693	693

various structural units changes slightly with the increase of MgO/Al<sub>2</sub>O<sub>3</sub> ratio, which may be related to the relatively small variations of compositions of slag.

The abundance of coexisting structural units in the molten slag is related to the corresponding band areas in the deconvoluted Raman spectra. Typically, the mole fractions of  $Q_{Si}^n$  species in the silicate network are calculated according to [40]

$$X_n = \frac{\theta_n A_n}{\sum_{n=0}^3 \theta_n A_n} \quad (2)$$

where  $X_n$ ,  $\theta_n$  and  $A_n$  denote the mole fraction of  $Q_{Si}^n$  species ( $n$  ranges from 0 to 3), Raman scattering coefficient and Raman band area of  $Q_{Si}^n$ , respectively. However, the exact values for  $\theta_n$  remain unknown. It is difficult to obtain the accurate abundances of structural units from Raman spectra. As an alternative, the relative variations of  $Q_{Si}^n$  can be analyzed by comparing the ratios of band area, by considering the  $\theta_n$  to be constant and only decided by  $Q_{Si}^n$  species themselves [33].

Figure 7(f) presents the variations of  $A_1/A_2$ ,  $A_3/A_2$  and  $A_0/A_2$  as a function of MgO/Al<sub>2</sub>O<sub>3</sub> ratio. It can be found that  $A_1/A_2$  and  $A_3/A_2$  have a decrease tendency when the MgO/Al<sub>2</sub>O<sub>3</sub> ratio is increased

from 0.82 to 1.36; whereas,  $A_0/A_2$  increases. This demonstrates that the complex silicate networks are modified and the degree of polymerization of silicate networks decreases. Furthermore, the area ratios of O—Ti—O deformations in sheet structure in the titanium-bearing structural units ( $S_1$ ) and [AlO<sub>4</sub>]-tetrahedral stretching vibrations in the aluminum-bearing structural units ( $S_2$ ) are also shown in Fig. 7(f). Clearly,  $S_1$  and  $S_2$  are decreased with an increase of MgO/Al<sub>2</sub>O<sub>3</sub> ratio. The complex O—Ti—O deformations in sheet structure and [AlO<sub>4</sub>]-tetrahedral stretching vibrations are depolymerized by forming the relatively simpler structural units, such as TiO<sub>4</sub><sup>4-</sup> monomers, Ti<sub>2</sub>O<sub>6</sub><sup>4-</sup> chains, Ti—O stretching vibrations in 6-coordinated Ti<sup>4+</sup> and [AlO<sub>6</sub>]-octahedron stretching vibration. This decreases the number of bridged oxygen in slag and weakens the degree of polymerization of titanium-bearing slag. Therefore, the viscosity and activation energy for viscous flow of slag decrease when the MgO/Al<sub>2</sub>O<sub>3</sub> ratio is increased in the experimental range. The depolymerization mechanisms of silicon-bearing structural units, aluminum-bearing structural units and titanium-bearing structural units are illustrated in Figs. 8, 9 and 10, respectively.

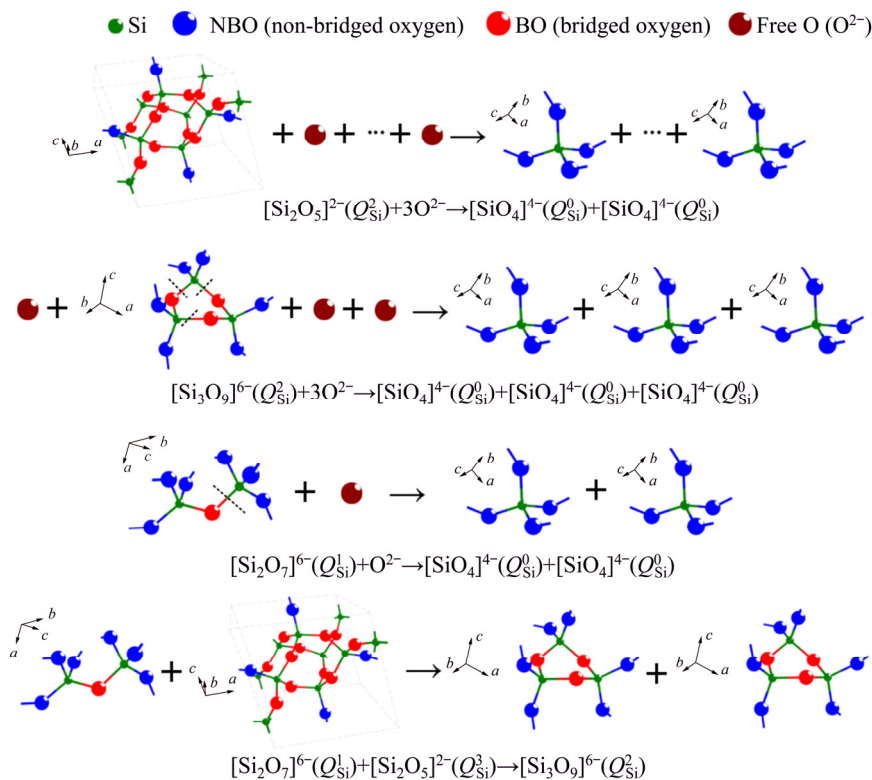


**Fig. 8** Depolymerizations of silicon-bearing structural units with MgO/Al<sub>2</sub>O<sub>3</sub> ratio

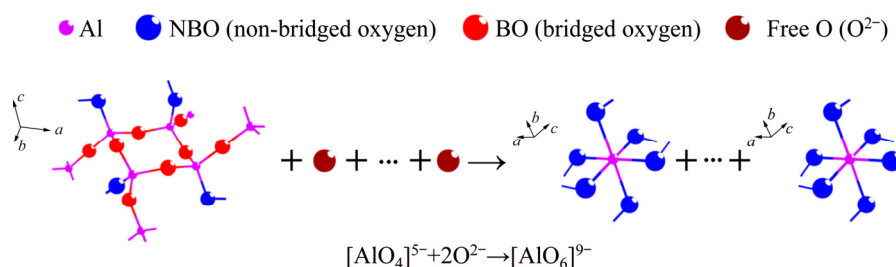


Fig. 9 Depolymerization of aluminum-bearing structural units with MgO/Al<sub>2</sub>O<sub>3</sub> ratio

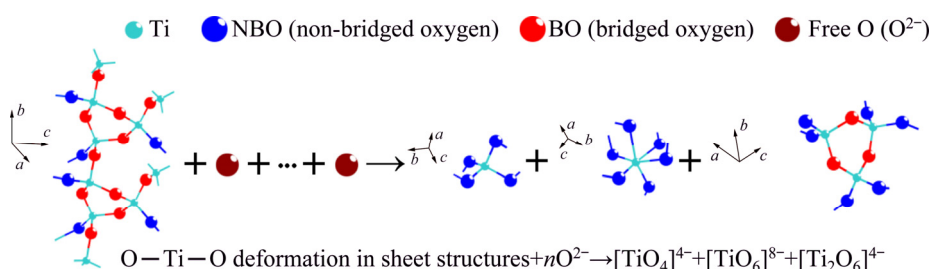


Fig. 10 Depolymerization of titanium-bearing structural units with MgO/Al<sub>2</sub>O<sub>3</sub> ratio

## 4 Conclusions

(1) When the MgO/Al<sub>2</sub>O<sub>3</sub> ratio is increased from 0.82 to 1.36, the viscosity and activation energy for viscous flow of MgO–Al<sub>2</sub>O<sub>3</sub>–TiO<sub>2</sub>–CaO–SiO<sub>2</sub> slag systems (TiO<sub>2</sub> content of 43 wt.% and CaO/SiO<sub>2</sub> ratio of 0.50) decrease, and the break point temperature initially decreases and subsequently increases.

(2) Raman spectroscopy results reveal that the complex silicate networks, O–Ti–O deformations in sheet structure and [AlO<sub>4</sub>]-tetrahedral stretching vibrations are depolymerized with the formations of simple structural units when the MgO/Al<sub>2</sub>O<sub>3</sub> ratio is increased. The degree of polymerization of titanium-bearing slag is weakened. The fluidity of slag has been improved.

(3) Calculated by Factsage 7.0, the liquidus temperature of experimental slags initially decreases and subsequently increases with the increase of MgO/Al<sub>2</sub>O<sub>3</sub> ratio, resulting in the same variations of break point temperature.

## References

- [1] LIU Shui-shi, GUO Yu-feng, QIU Guan-zhou, JIANG Tao. Solid-state reduction kinetics and mechanism of pre-oxidized vanadium–titanium magnetite concentrate [J]. Transactions of Nonferrous Metals Society of China, 2014, 24: 3372–3377.
- [2] WANG Ming-yu, WANG Xue-wen, HE Yue-hui, LOU Tai-ping, SUI Zhi-tong. Isothermal precipitation and growth process of perovskite phase in oxidized titanium bearing slag [J]. Transactions of Nonferrous Metals Society of China, 2008, 18: 459–462.
- [3] ZHAO Long-sheng, WANG Li-na, CHEN De-sheng, ZHAO Hong-xin, LIU Ya-hui, QI Tao. Behaviors of vanadium and chromium in coal-based direct reduction of high-chromium vanadium-bearing titanomagnetite concentrates followed by magnetic separation [J]. Transactions of Nonferrous Metals Society of China, 2015, 25: 1325–1332.
- [4] SUN Yu, ZHENG Hai-yan, DONG Yue, JIANG Xin, SHEN Yan-song, SHEN Feng-man. Melting and separation behavior of slag and metal phases in metallized pellets obtained from the direct-reduction process of vanadium-bearing titanomagnetite [J]. International Journal of Mineral Processing, 2015, 142: 119–124.
- [5] WANG Shuai, GUO Yu-feng, JIANG Tao, CHEN Feng, ZHENG Fu-qiang, YANG Ling-zhi, TANG Min-jun. Behavior of titanium during the smelting of vanadium titanomagnetite metallized pellets in an electric furnace [J]. JOM, 2019, 71: 323–328.
- [6] WU En-hui, ZHU Rong, YANG Shao-li, MA Lan, LI Jun, HOU Jing. Influences of technological parameters on smelting-separation process for metallized pellets of vanadium-bearing titanomagnetite concentrates [J]. Journal of Iron and Steel Research, International, 2016, 23: 655–660.
- [7] WANG Shuai, GUO Yu-feng, JIANG Tao, CHEN Feng, ZHENG Fu-qiang, TANG Min-jun, YANG Ling-zhi, QIU Guan-zhou. Appropriate titanium slag composition during smelting of vanadium titanomagnetite metallized pellets [J]. Transactions of Nonferrous Metals Society of China, 2018, 28: 2528–2537.
- [8] LI Yang, YU Hai-yang, ZHANG Zuo-tai, ZHANG Mei,

- GUO Min. Selective phase transformation behavior of titanium-bearing electric furnace molten slag during the molten NaOH treatment process [J]. *ISIJ International*, 2015, 55: 134–141.
- [9] LIU Ya-hui, MENG Fan-cheng, FANG Fu-qiang, WANG Wei-jing, CHU Jing-long. Preparation of rutile titanium dioxide pigment from low-grade titanium slag pretreated by the NaOH molten salt method [J]. *Dyes and Pigments*, 2016, 125: 384–391.
- [10] FENG Cong, CHU Man-sheng, TANG Jue, LIU Zheng-gen. Effects of smelting parameters on the slag/metal separation behaviors of Hongge vanadium-bearing titanomagnetite metallized pellets obtained from the gas-based direct reduction process [J]. *International Journal of Minerals, Metallurgy and Materials*, 2018, 25: 609–622.
- [11] KIM H, KIM W H, SOHN I, MIN D J. The effect of MgO on the viscosity of the CaO–SiO<sub>2</sub>–20wt.%Al<sub>2</sub>O<sub>3</sub>–MgO slag system [J]. *Steel Research International*, 2010, 81: 261–264.
- [12] KIM H, MATSUURA H, TSUKIHASHI F, WANG W, MIN D J, SOHN I. Effect of Al<sub>2</sub>O<sub>3</sub> and CaO/SiO<sub>2</sub> on the viscosity of calcium-silicate-based slags containing 10 mass pct MgO [J]. *Metallurgical and Materials Transactions B*, 2013, 44: 5–12.
- [13] SHI Cheng-bin, ZHENG Ding-li, SHIN S H, LI Jing, CHO J W. Effect of TiO<sub>2</sub> on the viscosity and structure of low-fluoride slag used for electros slag remelting of Ti-containing steels [J]. *International Journal of Minerals, Metallurgy and Materials*, 2017, 24: 18–24.
- [14] QIU Gui-bao, CHEN Long, ZHU Jian-yang, LV Xue-wei, BAI Chen-guang. Effect of Cr<sub>2</sub>O<sub>3</sub> addition on viscosity and structure of Ti-bearing blast furnace slag [J]. *ISIJ International*, 2015, 55: 1367–1376.
- [15] ZHEN Yu-lan, ZHANG Guo-hua, CHOU K C. Influence of Al<sub>2</sub>O<sub>3</sub>/TiO<sub>2</sub> ratio on viscosities and structure of CaO–MgO–Al<sub>2</sub>O<sub>3</sub>–SiO<sub>2</sub>–TiO<sub>2</sub> melts [J]. *ISIJ International*, 2014, 54: 985–989.
- [16] ZHANG Sheng-fu, ZHANG Xi, LIU Wei, LV Xue-wei, BAI Chen-guang, WANG Long. Relationship between structure and viscosity of CaO–SiO<sub>2</sub>–Al<sub>2</sub>O<sub>3</sub>–MgO–TiO<sub>2</sub> slag [J]. *Journal of Non-Crystalline Solids*, 2014, 402: 214–222.
- [17] LI Jiang-ling, SHU Qi-feng, CHOU K C. Structural study of glassy CaO–SiO<sub>2</sub>–CaF<sub>2</sub>–TiO<sub>2</sub> slags by Raman spectroscopy and MAS-NMR [J]. *ISIJ International*, 2014, 54: 721–727.
- [18] FENG Cong, TANG Jue, GAO Li-hua, LIU Zheng-gen, CHU Man-sheng. Effects of CaO/SiO<sub>2</sub> on viscous behaviors and structure of CaO–SiO<sub>2</sub>–11.00wt.%MgO–11.00wt.%Al<sub>2</sub>O<sub>3</sub>–43.00wt.%TiO<sub>2</sub> slag systems [J]. *ISIJ International*, 2019, 59: 31–38.
- [19] FENG Cong, CHU Man-sheng, TANG Jue, TANG Ya-ting, LIU Zheng-gen. Effect of CaO/SiO<sub>2</sub> and Al<sub>2</sub>O<sub>3</sub> on viscous behaviors of the titanium-bearing blast furnace slag [J]. *Steel Research International*, 2016, 87: 1274–1283.
- [20] FENG Cong, CHU Man-sheng, TANG Jue, QIN Jin, LI Feng, LIU Zheng-gen. Effects of MgO and TiO<sub>2</sub> on the viscous behaviors and phase compositions of titanium-bearing slag [J]. *International Journal of Minerals, Metallurgy and Materials*, 2016, 23: 868–880.
- [21] KIM G H, SOHN I. A study of the viscous properties with NaF additions in the CaO–SiO<sub>2</sub>–12 mass pct Na<sub>2</sub>O based slags [J]. *Metallurgical and Materials Transactions B*, 2011, 42: 1218–1223.
- [22] QI Jie, LIU Cheng-jun, JIANG Mao-fa. Role of Li<sub>2</sub>O on the structure and viscosity in CaO–Al<sub>2</sub>O<sub>3</sub>–Li<sub>2</sub>O–Ce<sub>2</sub>O<sub>3</sub> melts [J]. *Journal of Non-Crystalline Solids*, 2017, 475: 101–107.
- [23] LU Yu-fei. *Ironmaking technology* [M]. Beijing: Metallurgical Industry Press, 2010.
- [24] PARK J H, MIN D J, SONG H S. Amphoteric behavior of alumina in viscous flow and structure of CaO–SiO<sub>2</sub>(–MgO)–Al<sub>2</sub>O<sub>3</sub> slags [J]. *Metallurgical and Materials Transactions B*, 2004, 35: 269–275.
- [25] YAN Zhi-ming, LV Xue-wei, LIANG Dong, ZHANG Jie, BAI Chen-guang. Transition of blast furnace slag from silicates-based to aluminates-based: Viscosity [J]. *Metallurgical and Materials Transactions B*, 2017, 48: 1092–1099.
- [26] GAO Yun-ming, WANG Shao-bo, HONG Chuan, MA Xiu-juan, YANG Fu. Effects of basicity and MgO content on the viscosity of the SiO<sub>2</sub>–CaO–MgO–9wt.%Al<sub>2</sub>O<sub>3</sub> slag system [J]. *International Journal of Minerals, Metallurgy and Materials*, 2014, 21: 353–362.
- [27] KIM J B, SOHN I. Effect of SiO<sub>2</sub>/Al<sub>2</sub>O<sub>3</sub> and TiO<sub>2</sub>/SiO<sub>2</sub> ratios on the viscosity and structure of the TiO<sub>2</sub>–MnO–SiO<sub>2</sub>–Al<sub>2</sub>O<sub>3</sub> welding flux system [J]. *ISIJ International*, 2014, 54: 2050–2058.
- [28] ZHENG Kai, ZHANG Zuo-tai, LIU Li-li, WANG Xi-dong. Investigation of the viscosity and structural properties of CaO–SiO<sub>2</sub>–TiO<sub>2</sub> slags [J]. *Metallurgical and Materials Transactions B*, 2014, 45: 1389–1397.
- [29] WU Tuo, ZHANG Yan-ling, YUAN Fang, AN Zhuo-qing. Effects of the Cr<sub>2</sub>O<sub>3</sub> content on the viscosity of CaO–SiO<sub>2</sub>–10pctAl<sub>2</sub>O<sub>3</sub>–Cr<sub>2</sub>O<sub>3</sub> quaternary slag [J]. *Metallurgical and Materials Transactions B*, 2018, 49: 1719–1731.
- [30] DENG Lei-bo, ZHANG Xue-feng, ZHANG Ming-xing, JIA Xiao-lin. Effect of CaF<sub>2</sub> on viscosity, structure and properties of CaO–Al<sub>2</sub>O<sub>3</sub>–MgO–SiO<sub>2</sub> slag glass ceramics [J]. *Journal of Non-Crystalline Solids*, 2018, 500: 310–316.
- [31] ZHANG Lei, WANG Wan-lin, XIE Sen-lin, ZHANG Kai-xuan, SOHN I. Effect of basicity and B<sub>2</sub>O<sub>3</sub> on the viscosity and structure of fluorine-free mold flux [J]. *Journal of Non-Crystalline Solids*, 2017, 460: 113–118.
- [32] ZHENG Kai, LIAO Jun-lin, WANG Xi-dong, ZHANG Zuo-tai. Raman spectroscopic study of the structural properties of CaO–MgO–SiO<sub>2</sub>–TiO<sub>2</sub> slags [J]. *Journal of Non-Crystalline Solids*, 2013, 376: 209–215.
- [33] JIN Zhe-nan, YANG Hong-ying, LV Jian-fang, TONG Lin-lin, CHEN Guo-bao, ZHANG Qin. Effect of ZnO on viscosity and structure of CaO–SiO<sub>2</sub>–ZnO–FeO–Al<sub>2</sub>O<sub>3</sub> slags [J]. *JOM*, 2018, 70: 1430–1436.
- [34] MYSEN B, VIRGO D, SCARFE C. Relations between the anionic structure and viscosity of silicate melts—A Raman spectroscopic study [J]. *American Mineralogist*, 1980, 65: 690–710.
- [35] JUNG S S, SOHN I. Crystallization control for remediation of an Fe<sub>2</sub>O<sub>3</sub>-rich CaO–SiO<sub>2</sub>–Al<sub>2</sub>O<sub>3</sub>–MgO EAF waste slag [J]. *Environmental Science & Technology*, 2014, 48: 1886–1892.
- [36] MYSEN B, RYERSON F, VIRGO D. The influence of TiO<sub>2</sub>

- on the structure and derivative properties of silicate melts [J]. *American Mineralogist*, 1980, 65: 1150–1165.
- [37] PARK H, PARK J Y, KIM G H, SOHN I. Effect of  $\text{TiO}_2$  on the viscosity and slag structure in blast furnace type slags [J]. *Steel Research International*, 2012, 83: 150–156.
- [38] WANG Zhen, SHU Qi-feng, CHOU K C. Study on structure characteristics of  $\text{B}_2\text{O}_3$  and  $\text{TiO}_2$ -bearing F-free mold flux by Raman spectroscopy [J]. *High Temperature Materials and Processes*, 2013, 32: 265–273.
- [39] REYNARD B, GUYOT F. High-temperature properties of geikielite ( $\text{MgTiO}_3$ -ilmenite) from high-temperature high-pressure Raman spectroscopy—Some implications for  $\text{MgSiO}_3$ -ilmenite [J]. *Physics and Chemistry of Minerals*, 1994, 21: 441–450.
- [40] SUN Yong-qi, ZHANG Zuo-tai, LIU Li-li, WANG Xi-dong. FTIR, Raman and NMR investigation of  $\text{CaO-SiO}_2\text{-P}_2\text{O}_5$  and  $\text{CaO-SiO}_2\text{-TiO}_2\text{-P}_2\text{O}_5$  glasses [J]. *Journal of Non-Crystalline Solids*, 2015, 420: 26–33.

## MgO/Al<sub>2</sub>O<sub>3</sub> 比对 MgO–Al<sub>2</sub>O<sub>3</sub>–TiO<sub>2</sub>–CaO–SiO<sub>2</sub> 低碱度高钛渣黏流行为和结构的影响

冯 聪<sup>1,2</sup>, 高立华<sup>1,2</sup>, 唐 珏<sup>1,2</sup>, 柳政根<sup>1</sup>, 储满生<sup>1,2</sup>

1. 东北大学 冶金学院, 沈阳 110819;
2. 东北大学 轧制技术及连轧自动化国家重点实验室, 沈阳 110819

**摘 要:** 运用旋转柱体法分析 MgO/Al<sub>2</sub>O<sub>3</sub> 比对 MgO–Al<sub>2</sub>O<sub>3</sub>–TiO<sub>2</sub>–CaO–SiO<sub>2</sub> 渣系黏流行为的影响。采用拉曼光谱研究渣系结构特征, 结合 Factsage 7.0 热力学软件分析实验渣系液相线温度。结果表明, 当 MgO/Al<sub>2</sub>O<sub>3</sub> 比由 0.82 升高至 1.36 时, 渣系黏度和黏流活化能降低, 渣系熔化性温度和液相线温度先降低后升高, 渣中复杂黏滞结构逐渐解聚为简单黏滞流动单元。随 MgO/Al<sub>2</sub>O<sub>3</sub> 比升高, 实验渣系聚合程度降低, 实验渣系流动性得到改善, 使得渣系黏度和黏流活化能降低。此外, 渣系液相线温度随 MgO/Al<sub>2</sub>O<sub>3</sub> 比的变化导致渣系熔化性温度发生对应变化。

**关键词:** 钒钛磁铁矿; 含钛渣系; 黏流行为; 渣系聚合程度; MgO/Al<sub>2</sub>O<sub>3</sub> 比

(Edited by Bing YANG)